Angkasa Jurnal Ilmiah Bidang Teknologi
ISSN : 2085-9503 (Print)
ISSN : 2581-1355 (On Line)
Accredited Third Grade by Kemenristekdikti, Decree No: 10/C/C3/DT.05.00/2025
DOI : 10.28989/angkasa.v17i1.3074

Robust Stability of Sliding Mode Control for Pitch Attitude Boeing 747 Aircraft System

Paulus Setiawan[1,*], Lorenso Oldiardo Matuan[2], Yenni Astuti[3], Bambang Sudibya[4], Denny Dermawan[5], Freddy Kurniawan[6], Lasmadi[7]
[1,2,3,4,5,6,7]Program Studi Teknik Elektro, Institut Teknologi Dirgantara Adisutjipto

Article Info

Article history:

Received June 13, 2025
Accepted August 27, 2025
Published November 20, 2025

Keywords:

Pitch Attitude
Lead Compensator
Luenberger Observer
Sliding Mode Control (SMC)

ABSTRACT

The development of the aircraft's pitch-attitude control system starts by gathering data on its longitudinal motion, which is then translated into a mathematical transfer-function model describing the pitch-attitude dynamics. After the pitch attitude instability is identified, a compensator is intended to improve The ability to maintain stable pitch motion, and the compensator used in this study is a lead compensator. The drawback of this lead compensator is the settling time value which is still considered quite long and the peak overshoot value is also considered still quite high. In order to decrease the settling time and minimize the overshoot in the pitch-attitude control system, this study implements both the Luenberger observer control method and the Sliding Mode Control (SMC) technique. The results in this study show that at a positive 10-degree pitch attitude change, the system with the SMC controller shows a decrease in overshoot of 1,079.167% when compared to the lead compensator controller, the system with the SMC controller experiences a decrease in settling time value of 340.627% when compared to the Luenberger Observer controller.

Corresponding Author:

Paulus Setiawan,
Program Studi Teknik Elektro, Institut Teknologi Dirgantara Adisutjipto
Jl. Janti, blok R, Yogyakarta 55198, Indonesia.
Email: *paulussetiawan@itda.ac.id

1. INTRODUCTION

Generally, an aircraft experiences three straight-line motions (vertical, horizontal, and lateral) and three turning motions (pitch, roll, and yaw), which are managed using the elevators, rudder, and ailerons. Additionally, the aircraft's control system has the ability to be categorized organized as control in the longitudinal and lateral directions. With respect to longitudinal control, the elevator manages the aircraft's pitch or forward-backward motion. Positioned at the rear of the aircraft and aligned with the wings—where the ailerons are also located—the elevators are responsible for controlling the pitch. Pitch control falls under longitudinal dynamics, and this study focuses on designing an autopilot system to regulate the aircraft's pitch. An autopilot system governs an aircraft's trajectory without requiring constant manual input from the pilot. The autopilot assists the pilot rather than replacing them, and aids in controlling the aircraft, enabling the pilot to give attention to higher-level tasks such as monitoring the flight path, weather, and onboard systems [1]. A major challenge in flight control systems lies in managing the interplay of nonlinear dynamics, uncertainties from incomplete modeling, and variations in parameters when characterizing an aircraft and its operating conditions.

Research and analysis relating to a 3-DOF aircraft control and manipulation system for longitudinal dynamic computer-based flight simulation in a wind tunnel, the system comprises a manipulator arm with two independent motion parameters of rotation and the aircraft model located at the third joint, which only moves in the longitudinal direction (longitudinal and vertical motions), while The aircraft's pitch is unrestricted and

controllable through the moving tail. The aircraft dynamics model is utilized for generate dynamic behavior trajectories under free-flight conditions. The aircraft operation and control system is modeled with the Euler approach and controlled with PID to follow the trajectory. Reference angles for the manipulator are calculated via inverse kinematics. MATLAB/Simulink simulations are carried out, and the virtual flight test results are compared to the free-flight trajectory, demonstrating the system's applicability for virtual flight testing. [2].

research that analyzes guidance system for tracking UAV with nonlinear dynamics in discrete time dynamics experiencing uncertainty, time-variant perturbations, and input constraints, with a neural network approach, the system uncertainty is estimated, while the disturbance is resolved by means of a nonlinear discrete-time disturbance observer (DTDO). An adaptive neural control (ANC) strategy based on backstepping technique is developed using a supplementary system along with a tracking differentiator. Time Discrete Lyapunov analysis shows the stability of the signal in a closed system. That validity of the method is proven through numerical simulations [3].

This study analyzes the robust flight control for multirotor UAVs (MAVs) under limited force and torque disturbances, especially for MAVs with even number of fixed rotors (≥ 4). The approach used involves a hierarchical control architecture with quadratic programming-based control allocation independent of rotor configuration. Position and attitude controls are created separately through Fast Nonsingular Terminal Sliding Mode Control (FNTSMC) method to ensure guaranteed stability and robustness over a finite interval. The primary contributions include that extension belonging to the hierarchical control approach to all types of fixed-rotor MAVs and the stability analysis of FNTSMC. Simulation results and hardware tests demonstrate the effectiveness, flexibility, and reliability of the system under nonlinear and limited disturbance conditions [4].

This paper introduces an alternative that Sliding Mode Control (SMC) as a strong conventional velocity loop controller, which can effectively overcome the limitations associated with PI-based or lag compensator-based methods. SMC was introduced around the 1950s, where it is very advantageous applicable to nonlinear systems because of its invariant characteristics, which can ensure strong resilience to parameter uncertainties as well as external disturbances. Using controlling the mechanism state to follow a defined sliding interface, SMC enables fast transient performance and accurate control even in dynamic environments [5]. However, its inherent discontinuity can cause a phenomenon known as chattering, quick oscillatory behavior in the control mechanism signal that can reduce performance, induce oscillations in machinery, accelerate component wear, and compromise control precision. To address these issues, several improvements have been developed, including advanced sliding mode control, approaches in boundary layer theory, and smooth control approaches. From several literature reviews that have been mentioned, a grouping of control methods can be drawn where the lead compensator is included in the classical design method, then the state variable feedback is included into the state space method, and that sliding mode control is included in the optimal control system. So in this study the update proposed by the author is the control of the pitch attitude system using that sliding mode control (SMC) method, where that SMC method is then compared to the lead compensator and Luenberger observer methods.

2. RESEARCH METHODS

In conducting research and analysis of a system so that it can run well, there needs to be a sequence of methods that must be studied and explained. Some of these methods are expected to make research analysis easy to complete.

2.1. System Dynamics

To model an aircraft, it is necessary to derive the equations that represent its behavior. This is done by employing Newtonian mechanics to link external forces and moments to the resulting accelerations of the system. When modeling an aircraft system, certain assumptions need to be made, and specific axes must be chosen. Aircraft typically have three rotational movements and three translational movements. Aircraft motion is associated with two types of dynamics: lateral and longitudinal dynamics. The aircraft's pitching motion is regarded as its longitudinal dynamics, while the roll and yaw movements are categorized as its lateral dynamics. The yawing motion of an aircraft refers to its movement to the right or left around that z axis, even though that rolling motion involves the air vehicle rotating around that x axis, as illustrated in Figure 1.

In air vehicle modeling, six coupled the motion of the system is described by nonlinear equations employed within describe the aircraft's dynamics, consequently can be difficult to analyze. However, with certain assumptions, these nonlinear equations are simplified into two sets, each containing three mathematical expressions [6]. Three equations from the set of six represent the forces in the direction of the axes, while that remaining three describe that moment equations around that axes.

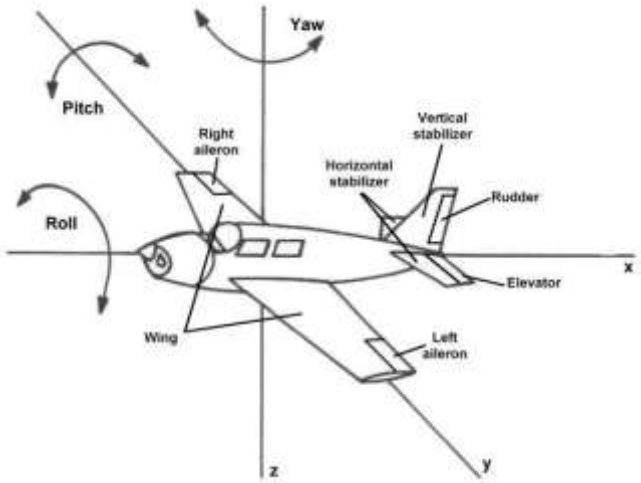

Figure 1. Aircraft coordinate system [1].

2.2. Transfer Function for Longitudinal Motion

The aircraft under consideration, a Boeing 747-400, is operating in steady, straight and level flight at an altitude of 20,000 feet featuring a speed of 673 ft/s, while the impact of compressibility is ignored. The values applicable to this aircraft are provided in that Table 1 and Table 2 below [7].

Table 1. Aircraft Stability Features

Aircraft	747-400
Parameters	
Altitude (ft)	20,000
Mach	0.650
True Speed (ft/s)	673
Dynamic Pressure $\left(lb/ft^2\right)$	287.2
Weight (lb)	636,636
Wing Area-S- $\left(ft^2\right)$	5,500
Wing Span-b-(ft)	196
Wing Chord-c-(ft)	27.3
C.G.(xc)	0.25
Trim AOA (deg)	2.5
$I_{xxs}\left(slugs-ft^2\right)$	$1.82x10^7$
$I_{yys}\left(slugs-ft^2\right)$	$3.31x10^7$
$I_{zzs}\left(slugs-ft^2\right)$	$4.97x10^7$
$I_{xzs}\left(slugs-ft^2\right)$	$-4.05x10^5$
Longitudinal Derivatives	
$X_u(1/s)$	-0.0059
$X_\alpha\left(ft/s^2\right)$	15.9787
$Z_u(1/s)$	-0.1104
$Z_\alpha\left(ft/s^2\right)$	-353.52
$M_u\left(1/ft.s\right)$	0
$M_\alpha\left(1/s^2\right)$	-1.3028
$M_{\dot{\alpha}}(1/s)$	-0.1057
$M_q(1/s)$	-0.5417
$X_{\delta e}\left(ft/s^2\right)$	0.0000
$Z_{\delta e}\left(ft/s^2\right)$	-25.5659
$M_{\delta e}\left(1/s^2\right)$	1.6937

 ISSN : 2085-9503 (Print), 2581-1355 (On Line)

Prior to conducting computations, it is necessary to determine several additional coefficients. These coefficients are derived from computer models instead of wind-tunnel experiments or real-world data, and they use axes aligned with stability.

Table 2. Extra Coefficients for the Aircraft

S	5500 ft^2	C_{Du}	0
$\bar{c}$	27.3 ft	$C_{D\alpha}$	0.2
b	196 ft	C_{TXu}	-0.055
h	20000ft	C_{Lo}	0.21
M	0.65	C_{Lu}	0.13
U_1	673 fps	$C_{L\alpha}$	4.4
$\bar{q}$	287.2 lb/ft^2	$C_{\dot{L}\alpha}$	7
CG	0.25%. $\bar{c}$	C_{Lq}	6.6
α_1	2.5 deg	C_{mo}	0
W	636636 lb/ft^2	C_{mu}	0.013
I_{xx}	18,200,000 slug. ft^2	$C_{m\alpha}$	-1
I_{yy}	33,100,000 slug. ft^2	$C_{\dot{m}\alpha}$	-4
I_{zz}	49,700,000 slug. ft^2	C_{mq}	-20.5
I_{xz}	970,000 slug. ft^2	C_{mTu}	0
C_{L1}	0.4	$C_{mT\alpha}$	0
C_{D1}	0.025	C_{DDe}	0
C_{TX1}	0.025	C_{LDe}	0.32
C_{m1}	0	C_{mDe}	-1.3
C_{MT1}	0	C_{Dih}	0
C_{Do}	0.0164	C_{lih}	0.7
C_{mih}	-2.7		

At low cruise conditions, stability derivatives are computed using mathematical techniques and solved to determine transfer functions, resistance to motion ratios, and natural frequencies for any value other than zero solutions, applying both the fast and slow flight motion mode approximations [8], [9]. The calculations are carried out to achieve any solution other than zero, and the measurements in the coefficient matrix A are determined as illustrated in Table 3 below.

Table 3. The Values in Coefficient Matrix A

X_u	-0.005930	$Z_{\delta e}$	-25.5453
X_{Tu}	-0.005930	M_u	0.0000251658
X_α	15.9658	M_{Tu}	0
$X_{\delta e}$	0	M_α	-1.30281
Z_u	-0.110314	$M_{T\alpha}$	0
Z_α	-355.239	$M_{\dot{\alpha}l}$	-0.105696
$Z_{\dot{\alpha}k}$	-11.3338	M_q	-0.541693

Z_q	-10.6862	$M_{\delta e}$	-1.69366

A solution with a nonzero value for the longitudinal equations of motion, expressed in matrix form are:

$$\begin{pmatrix} (s - X_u - X_{Tu}) & -X_\alpha & gCos(\theta) \\ -Z_u & (s(U - Z_\alpha) - Z_\alpha) & (-(Z_q + U)s + gSin[\theta]) \\ -(M_u + M_{Tu}) & -(M_\alpha s + M_\alpha + M_{T\alpha}) & (s^2 - M_q s) \end{pmatrix} \begin{pmatrix} u(s) \\ \alpha(s) \\ \theta(s) \end{pmatrix} = \begin{pmatrix} 0 \\ C_{z\delta e} \\ C_{M\delta e} \end{pmatrix} \quad (1)$$

A solution with a nonzero value for the longitudinal equations of motion, representated are:

$$\begin{pmatrix} 0.00652392 + s & -15.96582 & 32.174 \\ 0.110314 & 355.2394 + 684.334s & -662.314s \\ -0.0000251658 & 1.302818 + 0.105696196s & 0.541693s + s^2 \end{pmatrix} \begin{pmatrix} u(s) \\ \alpha(s) \\ \theta(s) \end{pmatrix} = \begin{pmatrix} 0 \\ -25.5453 \\ -1.69366 \end{pmatrix}$$

The calculation of transfer function of $\frac{\theta(s)}{\delta_e(s)}$:

$$\frac{\theta(s)}{\delta_e(s)} = \frac{-1.68971(0.0119211 + s)(0.486136 + s)}{(0.00465356 + 0.00453985s + s^2)(1.5423 + 1.16507s + s^2)}$$

And the state space system of $\frac{\theta(s)}{\delta_e(s)}$:

$$\begin{pmatrix} \dot{x}_1 \\ \dot{x}_2 \\ \dot{x}_3 \\ \dot{x}_4 \end{pmatrix} = \begin{pmatrix} -1.1696 & -1.5545 & -0.0124 & -0.0072 \\ 1 & 0 & 0 & 0 \\ 0 & 1 & 0 & 0 \\ 0 & 0 & 1 & 0 \end{pmatrix} \begin{pmatrix} x_1 \\ x_2 \\ x_3 \\ x_4 \end{pmatrix} + \begin{pmatrix} 1 \\ 0 \\ 0 \\ 0 \end{pmatrix} u$$

$$y = \begin{pmatrix} 0 & 1 & 0.8416 & 0.0098 \end{pmatrix} \begin{pmatrix} x_1 \\ x_2 \\ x_3 \\ x_4 \end{pmatrix}.$$

The dynamic system represented by state space equations is shown in Figure 2.

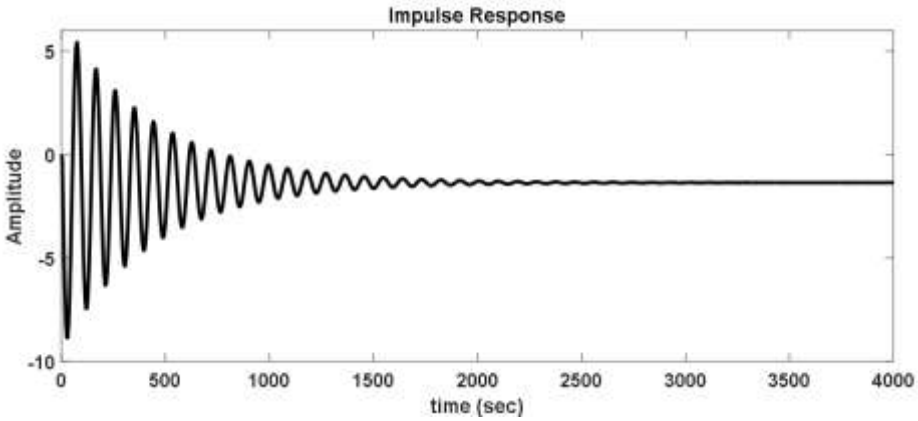

Figure 2. Transient response of the pitch attitude aircraft.

The aircraft's longitudinal dynamics nonlinear equations have been approximated linearly using perturbation analysis for small deviations, resulting in that derivation of the aircraft transfer function of pitch system based on the assumptions made as discussed earlier. The aircraft's pitch system is observed to be stable, as the system's poles are located in the left portion of that s-plane [10]. Therefore, the of the control is to ensure the system meets its operational requirements, which include tracking the step command with a transition time of below 16 seconds and a peak overshoot of below 0.25%. Additionally, the response of the system must reach the ultimate settled value within 40 seconds, with a steady-state error of less than 2%. In order to meet the defined control objectives and further enhance that stability of the pitch dynamics system of the aircraft, this paper discusses three control methodologies: lead compensator, Luenberger observer, and sliding mode control (SMC).

2.3. Lead Compensator Controller

 ISSN : 2085-9503 (Print), 2581-1355 (On Line)

For lead networks, the transfer function is (without featuring a gain constant) is represented as:

$$G_c(s) = \frac{1+\tau s}{1+\tau s/\alpha} \tag{2}$$

If the frequency response of the open-loop system analysis indicates with positive contributions to gain and phase from $G_c(s)$ are required to attain the intended ω_c and ψ, a lead network can then be used to achieve the specified dynamic response. The gain equations (dB) and contribution to phase of (ϕ) to G_c exist as follows:

$$p = \tan\Phi = \frac{\omega\tau - (\omega\tau/\alpha)}{1+(\omega\tau)^2/\alpha} \tag{3}$$

$$dB = 10\log\left[\frac{1+(\omega\tau)^2}{1+(\omega\tau/\alpha)^2}\right]; \text{ or}$$

$$c = 10^{dB/10} = \left((1+\omega\tau)^2\right)/\left((1+\omega\tau/\alpha)^2\right) \tag{4}$$

Solving results in $\alpha^2(\alpha-1)^2\left[(p^2-c+1)\alpha^2+2p^2c\alpha+p^2c^2+c^2-c\right]=0$ (5)

Given that there are multiple roots at zero and 1 are unsuitable for the design, the value of α must be positive. It is straightforward to demonstrate that for a single compensation network $c > p^2+1$. Once this requirement is satified, that quadratic equation will produce both one positive and one negative solution. The valid value for α is positive. By means of ω_c and α, τ could be computed using the magnitude expression of (2), expressed with follow:

$$(\omega\tau)^2 = \frac{\alpha^2-\alpha^2 c}{c-\alpha^2} \tag{6}$$

The above procedure is straightforward, precise, and reliable. However, if the accuracy of the graph reading is adequate, the solution may be found without requiring computations [11]. The graphs are plotted using the required phase and gain contributions, as illustrated in Figure 3, Figure 4, and Figure 5. The magnitudes of $\omega\tau$ and α are obtained by interpolating the parameterized curves. Damping coefficient ratio (ξ): 0.8843; overshoot: -0.247%; Pole: -0.0688 ± j0.0367.

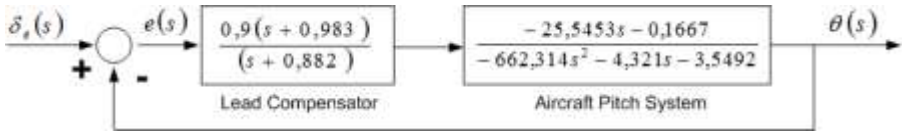

Figure 3. controller using lead compensation

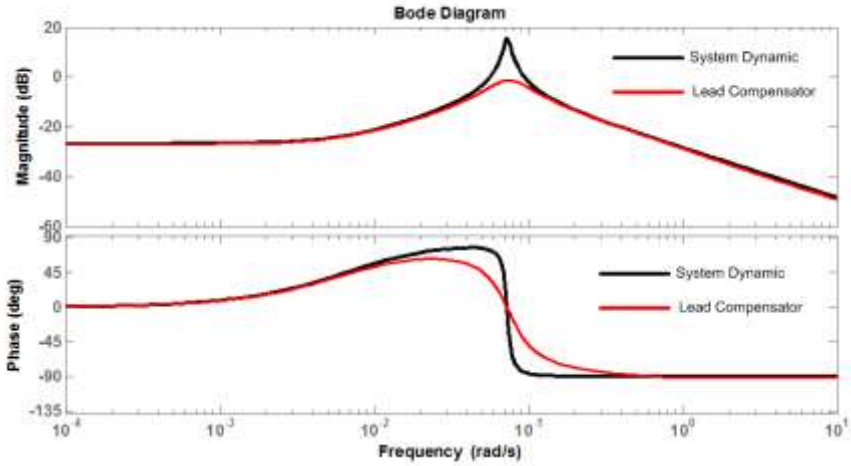

Figure 4. Magnitude response plot for $\frac{\theta(s)}{\delta_e(s)}$ transfer function versus ω for $s=j\omega$

2.4. Luenberger Observer Controller

The system is able to be represented with a collection of differential equations within the following configuration

$$\dot{x} = Ax + Bu + w \quad (7)$$
$$y = Cx + v$$

Examine the system defined by the collection of equations (7). Since the quantity of measurements is smaller compared to the count of phase coordinates. That is essential for specifying the filter in order to reduce the error rate $\varepsilon = x - \hat{x}$. Select a parameter p(t) as an indicator of the unobserved variables $p(t) = C'x(t)$, where C' represents the variable matrix that need to be rebuilt. Next, using the relation

$$y(t) = Cx(t)$$
$$p(t) = C'x(t)$$

It consequently the complete condition of the system $\hat{x}$ can be expressed as

$$\hat{x}(t) = \begin{pmatrix} C \\ C' \end{pmatrix}^{-1} \begin{pmatrix} y(t) \\ p(t) \end{pmatrix}$$

That is helpful to express the preceding equation in the form below

$$\begin{pmatrix} C \\ C' \end{pmatrix} = (L_1, L_2), \text{ so that } \hat{x}(t) = L_1 y(t) + L_2 p(t)$$

It is possible for p(t) to be determined using the differential equation below

$$\hat{p}(t) = C'Ax(t) + C'Bu(t) \text{ or}$$
$$\hat{p}(t) = C'AL_2 p(t) + C'AL_1 y(t) + C'Bu(t) \quad (8)$$

As shown in the equation, y(t) represents the input variable.

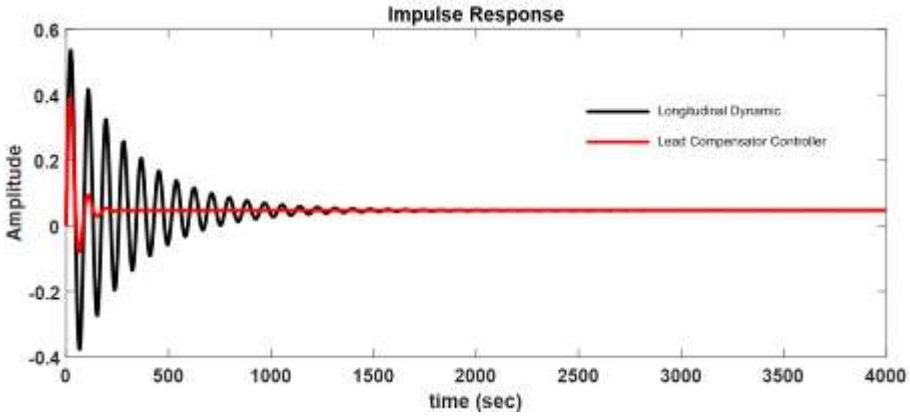

Figure 5. Pitch behavior of the aircraft using a phase-lead controller

For designing the reduced-order observer without specifying differentials (which are required to acquire further information), assume that

$$q(t) = \hat{p}(t) - Ky(t) \quad (9)$$

Equations (7) and (8) demonstrate is q(t) fulfills the equation involving derivatives

$$q(t) = [C'AL_2KCAL_2]q(t) + [C'AL_2K + C'AL_1$$
$$- KCAL_1 - KCAL_1K]y(t) + [CB - KCB]u(t)$$

The recovered state vector of the system appears as follows

$$\hat{x}(t) = L_2 q(t) + (L_1 + L_2 K)y(t) \quad (10)$$

Equations (8) and (10) outline the lower-order observer. To transform the continuous observer defined by (8) and (9) into a discrete form, assume that

$\dot{x} \approx \frac{x_n - x_{n-1}}{T}$, with T representing the sampling time.

A framework is considered observable if it can fully recover its state from the measured output value. The state observer can determine the inner states of that system using the observed system's input and output values [12], [13]. The monitoring system for the time-varying system, derived from the Luenberger observer, is illustrated in Figure 6.

 ISSN : 2085-9503 (Print), 2581-1355 (On Line)

$$A=\begin{pmatrix}-1.1696 & -1.5545 & -0.0124 & -0.0072\\ 1 & 0 & 0 & 0\\ 0 & 1 & 0 & 0\\ 0 & 0 & 1 & 0\end{pmatrix};\ B=\begin{pmatrix}1\\0\\0\\0\end{pmatrix};C=\begin{pmatrix}0 & 1 & 0.8416 & 0.0098\end{pmatrix}$$

$$j=\begin{pmatrix}-0.583+j1.1 & -0.583-j1.1 & -0.02 & -0.83\end{pmatrix};$$

$$K=\begin{pmatrix}0.8464 & 1.0031 & 1.3244 & 0.0185\end{pmatrix};K_e=\begin{pmatrix}11.76\\8.53\\3.22\\17.41\end{pmatrix}$$

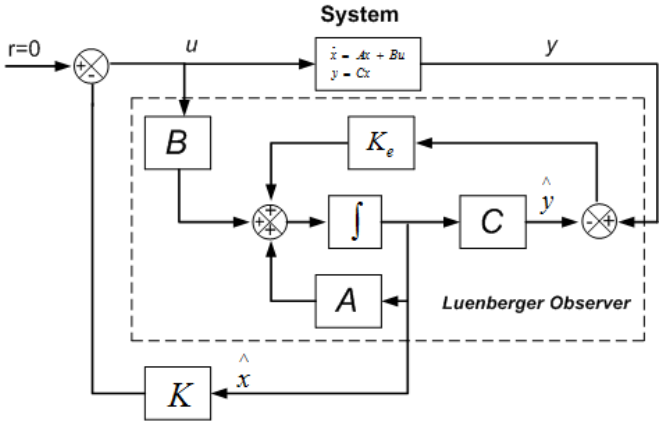

Figure 6. Luenberger Observer

2.5. Sliding Mode Control

SMC was established in the 1970s in the USSR, primarily intended for use in aerospace and weapons-missile systems [14], [15]. While grasping the precise mathematical details of the approach may be difficult, in numerous instances, SMC can be applied effectively without a thorough understanding of its complex mathematical foundation. Due to its robustness and these benefits, it is extensively applied in areas like applications in servo-drive, robotics, and power electronics systems, where system structures tend to change prevalent.

The objective of SMC is intended to steer the system to a condition where its motion characteristics are controlled using a differential equation that has reduced degrees range of motion. Within this state, the system is theoretically unaffected by changes in specific variables and specific kinds caused by outside disturbances. This situation is referred to as sliding behavior. While sliding mode control is theoretically considered an effective and robust control method, its practical implementation is unfortunately hindered by significant limitations. The primary issue is known as chattering [16], which refers to fast-varying oscillations in the vicinity of the sliding surface which greatly diminish the performance and reliability of the controller.

While SMC theoretically provides better performance for the closed-loop system operating in sliding mode, its practical constraints prevent some researchers. A key limiting factor is the requirement for an increased sampling rate compared to alternative control methods to suppress high-frequency oscillations (rapid switching). Several strategies can be used to tackle this issue, for example observer-based, discrete-time sliding mode control designs, which prevent the system from reaching critical region [17], [18].

That initial a step in developing a sliding-mode controller involves defining the sliding surface, which represent defined in the following way:

$$s=\left(\frac{de(t)}{dt}+C\times e(t)\right)^{n-1} \tag{11}$$

s represents the control surface, C represent a positive constant which defines that system's frequency range (sometimes referred to considered as λ in certain research), n serve as the system's level, and e denotes the error signal. For the brushed DC motor, the transfer function is of moment order, thus by replacing the speed, the sliding surface can be expressed in the following way:

$$s=\frac{d\omega_e(t)}{dt}+C\times\omega_e \tag{12}$$

The angular velocity ω_e represents the error signal, which is the difference between the reference signal and the process variable. After determining once the sliding surface is defined, the next step is to generate a command signal that allows the sliding surface to be reached and sustained. This is constrained by:

$$s \bullet \dot{s} > 0 \tag{13}$$

In order to meet this condition, the discontinuous controller output signal is derived using the sign (sgn) function, in which the variable denotes the current value of the sliding surface, with K being a positive constant:

$$u = K \times \text{sgn}(s) \tag{14}$$

The sign function (sgn) in the given equation (14) is described as:

$$s = \begin{cases} -1, s < 0 \\ +1, s \geq 0 \end{cases} \tag{15}$$

The sign (sgn) function can cause chattering, which may negatively impact the motor. Therefore, preventing this phenomenon is crucial for sliding mode control (SMC), as illustrated in Figure 7. One approach to avoid chattering, the sign function can be substituted with the pseudo function:

$$u = K \bullet \frac{s}{|s| + \delta} \tag{16}$$

Here, d represents a small positive constant known as an adjustabla parameter, which helps reduce chattering. That selection of d is an important factor, as choosing a value that is too small may still result in chattering, while a value that is too large could cause issues for the controller in reaching the reference value. The dynamic system, derived from sliding mode control (SMC), is illustrated in Figure 7.

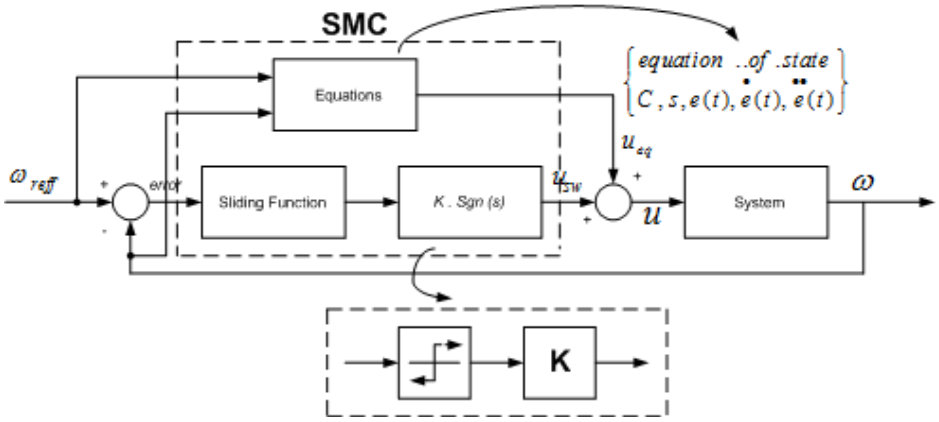

Figure 7. Block schema of SMC [19]

3. RESULTS AND DISCUSSION

In this present study, a simulation of pitch attitude control on a Boeing B747-400 aircraft will be conducted using the SMC method on Matlab simulink. Where with this SMC method, the performance of dynamic changes in the response flight control will be compared with the performance of the lead compensator method and the Luenberger observer method. Analysis of the response pitch attitude flight control will be carried out at the initial state, then when there is a growth in the positive degree magnitude and a decrease in the negative degree magnitude at that steady state position.

3.1. Comparison of Control Responses at Initial State

By referencing equations (10) to (15), constants like C, K, and δ can derive, which are then used to design the SMC system as presented in Figure 8, Figure 9, and Figure 10, specifically: $C = 3866{,}733$; $K = 91{,}48$; and $\delta = 84{,}19$. The simulation shown in Figure 8 is a system at the initial state which indicates that the system's state responds after receiving the SMC controller exhibited reduced overshoot of 734,043% when compared to the lead compensator controller [19], [20], namely from an amplitude value of 0,392 to 0,047. While the system with the SMC controller experienced a decrease in overshoot of 457,447% when compared to the Luenberger observer controller, namely from an amplitude value of 0,262 to 0,047. Then if the system is analyzed by measuring the settling time value, then the system with the SMC controller experienced a decrease in settling time value of 3.676,042% when compared to the lead compensator controller, namely from a time value of 290 seconds to 7,68 seconds. While the system with the SMC controller

 ISSN : 2085-9503 (Print), 2581-1355 (On Line)

experienced a decrease in settling time value of 1.501,563% when compared to the Luenberger observer controller, namely from a time value of 123 seconds to 7,68 seconds.

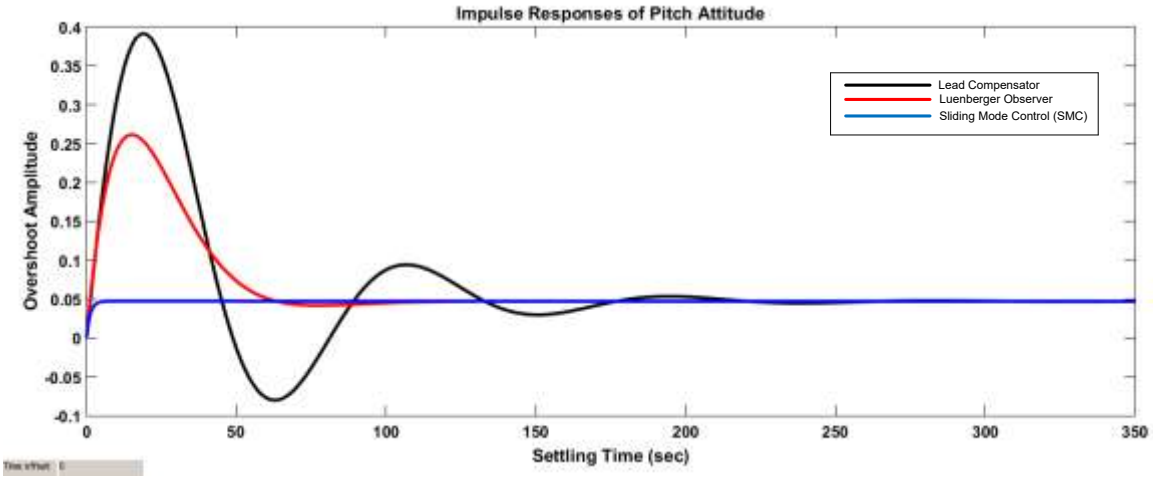

Figure 8. Comparison of control responses at initial state.

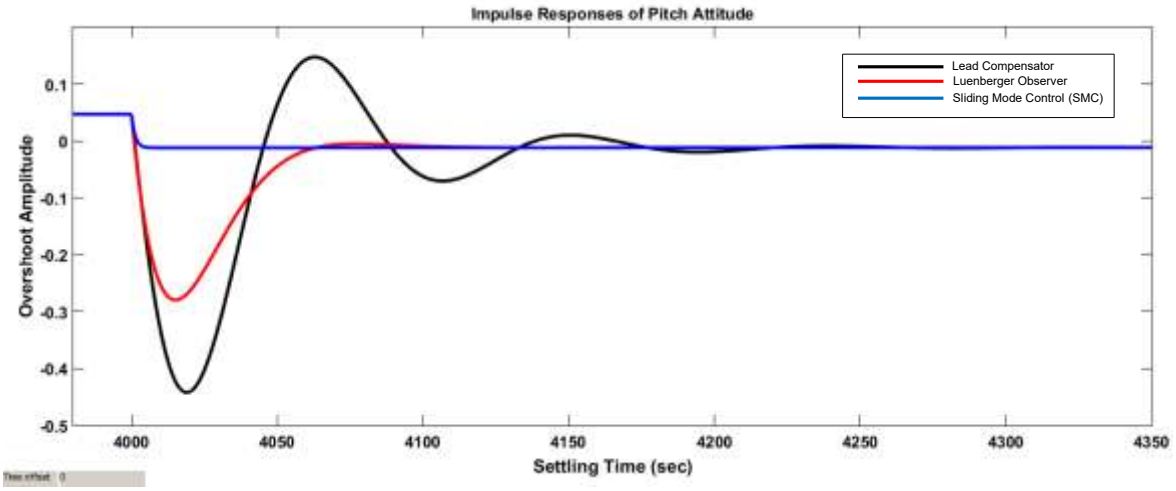

Figure 9. Change of direction manoeuvre -10 degree.

3.2. When a Negative Change in Direction Occurs

The simulation shown in Figure 9 illustrates a system undergoing a 10 degree negative pitch attitude change. In this scenario, the system with the SMC controller exhibits a 3.591,667% reduction in overshoot compared to the lead compensator controller, with the amplitude dropping from -0,443 to -0,012. Similarly, the system with the SMC controller shows a 2.233,33% decrease in overshoot compared to the Luenberger observer controller, with the amplitude reducing from -0,28 to -0,012. Additionally, when analyzing the settling time, the system with the SMC controller demonstrates a 1.186,207% reduction in settling time compared to the lead compensator controller, from 4373 seconds to 4029 seconds. The same 375,862% decrease in settling time is observed when comparing the SMC controller to the Luenberger observer controller, with the settling time also decreasing from 4138 seconds to 4029 seconds. In reference [5], the results show that the SMC approach delivers better dynamic behavior, quicker time to reach steady state, more seamless transitions, and improved stable state accuracy than Luenberger observer method.

3.3. When a Positive Change in Direction Occurs

The simulation depicted in Figure 10 demonstrates a system undergoing a 10-degree positive pitch attitude change. In this case, the system with the SMC controller shows a 1.079,167% reduction in overshoot compared to the lead compensator controller, with the amplitude decreasing from 0,283 to 0,024. Likewise, the system with the SMC controller experiences a 670,83% reduction in overshoot compared to the Luenberger observer controller, with the amplitude dropping from 0,185 to 0,024. Furthermore, in terms of settling time,

the SMC-controlled system exhibits a 1.051% decrease in settling time compared to the lead compensator controller, reducing from 8368 seconds to 8032 seconds. A similar 340,627% reduction in settling time is observed when comparing the SMC controller to the Luenberger observer controller, with the settling time decreasing from 8141 seconds to 8032 seconds.

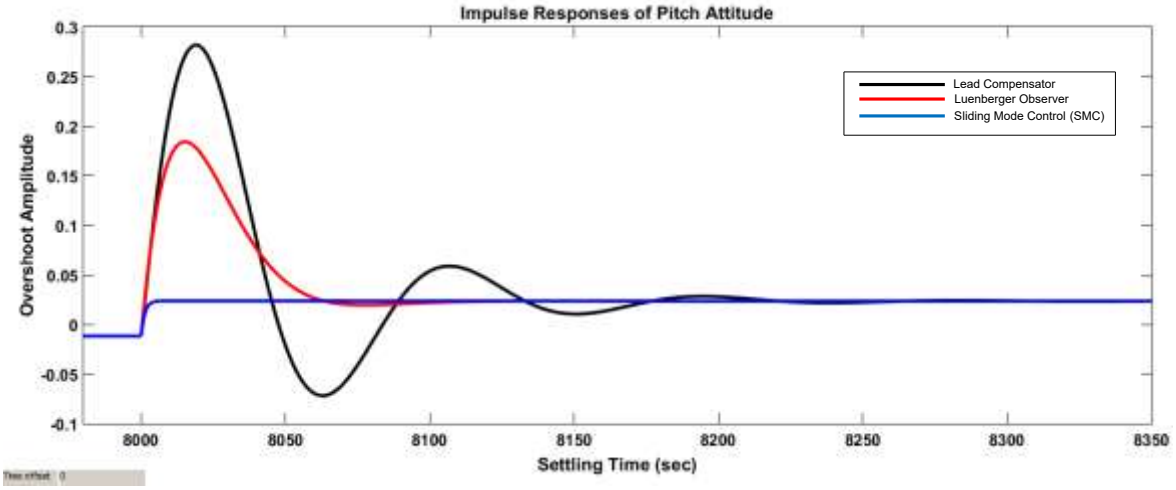

Figure 10. Change of direction manoeuvre +10 degree.

4. CONCLUSION

In this study, pitch attitude control on the flight control system with the sliding mode control (SMC) method can provide better and more optimal results when compared to the lead compensator and Luenberger observer methods. This is indicated by a low overshoot value and a faster settling time when compared to the two methods. At the beginning of a system moving then experiencing a positive degree value change and also experiencing a negative degree value change, the pitch attitude control system with the SMC method also provides optimal results when compared to the two methods mentioned previously. The results in this study show that at a positive 10-degree pitch attitude change, the system with the SMC controller shows a decrease in overshoot of 1,079.167% when compared to the lead compensator controller, and the system with the SMC controller experiences a decrease in settling time value of 340.627% when compared to the Luenberger Observer controller. The suggestion for future research is that it needs to be further analyzed if a dynamic flight control system is combined together between 3 axes, namely pitch, roll, and yaw so that the control system used becomes multi-input and multi-output.

REFERENCE

[1] A. Khalid, K. Zeb, and A. Haider, "Conventional PID, adaptive PID, and sliding mode controllers design for aircraft pitch control," *2019 International Conference on Engineering and Emerging Technologies, ICEET 2019*, pp. 1–6, 2019, doi: 10.1109/CEET1.2019.8711871.

[2] A. A. Ishola, J. F. Whidborne, and G. Tang, "An Aircraft-Manipulator System for Virtual Flight Testing of Longitudinal Flight Dynamics," *Robotics*, vol. 13, no. 12, pp. 1–15, 2024, doi: 10.3390/robotics13120179.

[3] S. Shao, M. Chen, and Y. Zhang, "Adaptive Discrete-Time Flight Control Using Disturbance Observer and Neural Networks," *IEEE Trans Neural Netw Learn Syst*, vol. 30, no. 12, pp. 3708–3721, 2019, doi: 10.1109/TNNLS.2019.2893643.

[4] A. L. Silva and D. A. Santos, "Fast Nonsingular Terminal Sliding Mode Flight Control for Multirotor Aerial Vehicles," *IEEE Trans Aerosp Electron Syst*, vol. 56, no. 6, pp. 4288–4299, 2020, doi: 10.1109/TAES.2020.2988836.

[5] M. Mamashli and M. Jamil, "Enhanced Dynamic Control for Flux-Switching Permanent Magnet Machines Using Integrated Model Predictive Current Control and Sliding Mode Control †," *Energies*, vol. 18, no. 5, 2025, doi: 10.3390/en18051061.

[6] P. Setiawan, D. Dermawan, F. Kurniawan, N. A. Purnami, R. Alriavindra Funny, and M. A. Deny Kusumaningrum, "Comparison of Robust Stability for Pitch Attitude Boeing 747 Aircraft System Based on LQG and Observer Controller," *Proceedings - IEIT 2023: 2023 International Conference on Electrical and Information Technology*, pp. 126–132, 2023, doi: 10.1109/IEIT59852.2023.10335591.

[7] D. Izci, S. Ekinci, A. Demiroren, and J. Hedley, "HHO Algorithm based PID Controller Design for Aircraft Pitch Angle Control System," *HORA 2020 - 2nd International Congress on Human-Computer Interaction, Optimization and Robotic Applications, Proceedings*, pp. 31–36, 2020, doi: 10.1109/HORA49412.2020.9152897.

[8] A. Ashraf, W. Mei, L. Gaoyuan, M. M. Kamal, and A. Mutahir, "Linear Feedback and LQR Controller Design for Aircraft Pitch Control," *2018 IEEE 4th International Conference on Control Science and Systems Engineering, ICCSSE 2018*, pp. 276–278, 2018, doi: 10.1109/CCSSE.2018.8724780.

[9] C. Radhakrishnan and A. Swarup, "Improved aircraft performance using simple pitch control," *2020 1st International Conference on Power, Control and Computing Technologies, ICPC2T 2020*, pp. 295–299, 2020, doi: 10.1109/ICPC2T48082.2020.9071452.

[10] C. Radhakrishnan and A. Swarup, "Performance Comparison for Fuzzy based Aircraft Pitch using Various Control Methods," *Proceedings of the 2nd International Conference on Inventive Research in Computing Applications, ICIRCA 2020*, pp. 428–433, 2020, doi: 10.1109/ICIRCA48905.2020.9183199.

[11] H. Okajima, K. Arinaga, and A. Hayashida, "Design of Observer-Based Feedback Controller for Multi-Rate Systems With Various Sampling Periods Using Cyclic Reformulation," *IEEE Access*, vol. 11, no. November, pp. 121956–121965, 2023, doi: 10.1109/ACCESS.2023.3329117.

[12] H. Min, S. Xu, Q. Ma, B. Zhang, and Z. Zhang, "Composite-Observer-Based Output-Feedback Control for Nonlinear Time-Delay Systems With Input Saturation and Its Application," *IEEE Transactions on Industrial Electronics*, vol. 65, no. 7, pp. 5856–5863, 2018, doi: 10.1109/TIE.2017.2784347.

[13] M. Hammouche, A. Mohand-Ousaid, P. Lutz, and M. Rakotondrabe, "Robust Interval Luenberger Observer-Based State Feedback Control: Application to a Multi-DOF Micropositioner," *IEEE Transactions on Control Systems Technology*, vol. 27, no. 6, pp. 2672–2679, 2019, doi: 10.1109/TCST.2018.2865767.

[14] J. M. Kiss, P. T. Szemes, and P. Aradi, "Sliding mode control of a servo system in LabVIEW: Comparing different control methods," *International Review of Applied Sciences and Engineering*, vol. 12, no. 2, pp. 201–210, 2021, doi: 10.1556/1848.2021.00250.

[15] K. K. D. Young, "Controller Design for a Manipulator Using Theory of Variable Structure Systems," *IEEE Trans Syst Man Cybern*, vol. 8, no. 2, pp. 101–109, 1978, doi: 10.1109/TSMC.1978.4309907.

[16] V. Utkin and H. Lee, "Chattering problem in sliding mode control systems," *Analysis and Design of Hybrid Systems 2006*, p. 1, 2006, doi: 10.3182/20060607-3-it-3902.00003.

[17] U. Kotta, "Comments on 'On the Stability of Discrete-Time Sliding Mode Control Systems,'" *IEEE Trans Automat Contr*, vol. 34, no. 9, pp. 1021–1022, 1989, doi: 10.1109/9.35824.

[18] P. Korondi, H. Hashimoto, and V. Utkin, "Direct torsion control of flexible shaft in an observer-based discrete-time sliding mode," *IEEE Transactions on Industrial Electronics*, vol. 45, no. 2, pp. 291–296, 1998, doi: 10.1109/41.681228.

[19] E. H. Dursun and A. Durdu, "Speed Control of a DC Motor with Variable Load Using Sliding Mode Control," *International Journal of Computer and Electrical Engineering*, vol. 8, no. 3, pp. 219–226, 2016, doi: 10.17706/ijcee.2016.8.3.219-226.

[20] M. Jamil, A. Waris, S. O. Gilani, B. A. Khawaja, M. N. Khan, and A. Raza, "Design of Robust Higher-Order Repetitive Controller Using Phase Lead Compensator," *IEEE Access*, vol. 8, pp. 30603–30614, 2020, doi: 10.1109/ACCESS.2020.2973168.